Variations of fluvial tufa sub-environments in a tectonically active basin, Pleistocene Teruel basin, NE Spain

Jon Camuera [a], Ana M. Alonso-Zarza [b,c], Álvaro Rodríguez-Berriguete [b,c], Alfonso Meléndez [d]

[a] Department of Stratigraphy and Paleontology, Faculty of Science, University of Granada. Fuentenueva s/n Av., 18002, Granada, Spain.

[b] Department of Petrology and Geochemistry, Faculty of Geological Science, University Complutense Madrid. José Antonio Novais 12 St., 28040, Madrid, Spain.

[c] Institute of Geosciences, UCM-CSIC. José Antonio Novais 12 St., 28040, Madrid, Spain.

[d] Department of Earth Sciences, University of Zaragoza. Pedro Cerbuna 12 St., 50009, Zaragoza, Spain.

* Corresponding Author's telephone number and email: 653710139 / jcamuera@ugr.es

KEYWORDS: fluvial tufa, Teruel basin, tectonism, Pleistocene, isotopes

ABSTRACT

The Pleistocene Tortajada fluvial deposit occurs in the eastern active margin of the Teruel Basin. It developed in the early stages of opening of the basin and at present is disconnected to the Alfambra River. The preserved deposits show that the fluvial systems consisted in three different sub-environments including: Upper Terraces, Ponds and Cascades. The main facies are framestones of stems, phytoclastic rudstone, framestone of bryophytes, peloidal and filamentous stromatolites, mudstone and detrital (conglomerates and slope-breccias) facies. These facies are arranged in three different sequence types, all of them showing a lower detrital term followed by pond and, in cases, cascade deposits. The microfacies analyses reveal that both biotic and abiotic processes performed an important role in the deposition within the river. Isotopic analyses ($\delta^{18}O$ from -8.58‰ to -6.70‰ VPDB and $\delta^{13}C$ from -7.44‰ to -3.97‰ VPDB) are indicative of meteoric water within a hydrologically open system. The carbonate hinterland rocks, together with a semi-arid to sub-humid climate favored carbonate accumulation within the river.

Our results point out that the location, morphology and sedimentary sequences of the Tortajada fluvial systems had an important tectonic control. The situation of the main and secondary faults controlled the paleomorphology of the river floor. Thus cascades are found in areas of important step faults, whereas the spaces between faults were occupied by fluviatile/lacustrine areas. In addition the development of the different sedimentary sequences was also a reflection of movements of these faults. In short, our study may confirm that tectonism is an important control on tufa development.

1. Introduction

Tufas are freshwater carbonates which contain remains of micro- and macrophytes that have been coated and/or impregnated by carbonate (Ford and Pedley, 1996; Arenas et al., 2010b). Unlike their thermogene travertine counterparts which are mostly fed by deep hydrothermal waters (Pentecost, 2005), tufas are mainly fed by meteoric waters (Pentecost and Viles, 1994; Ford and Pedley, 1996; Gandin and Capezzuoli, 2008). Fluvial tufas have been the aim of a variety of sedimentological, geomorphological, hydrological or biological studies (Ordóñez and García-del-Cura, 1983; Pedley, 2009). These carbonate deposits are related with rivers currently active in both water circulation and carbonate deposition in valleys (Peña et al., 2000; Pedley et al., 2003;

Luzón et al., 2011). They have a great potential as paleoenvironmental archives, especially as paleoclimatic indicators (Andrews et al., 2000; Andrews, 2006), as tufa formation is favored during warm and humid interglacial periods in which water availability is higher (Capezzuoli et al., 2010; Pazzaglia et al., 2013). In many cases, continuous tufa formation in Quaternary fluvial systems is linked with periods/basins of tectonic quiescence, with no significant changes in morphology except those related with the entrenchment of the fluvial system. However, various studies have pointed out the close relationships of travertines with active faults, especially in extensional settings (Barnes et al., 1978; Hancock et al., 1999). This is because: 1) faults and fractures are efficient conduits for fluid migration (Hancock et al., 1999; Özkul et al., 2013; Özkul et al., 2014), 2) fault activity can increase water velocity and so favour mechanical water outgassing, triggering calcite precipitation (Ordóñez and García-del-Cura, 1983; Peña et al., 2000) and 3) the topographic expression of tectonic movements in the surface can create favourable morphologies for tufa deposition. The result is that a number of travertine occurrences are situated in the nearby of active fault systems, mostly in the hanging walls of extensional basins (Muir-Wood, 1993, Hancock et al., 1999). This association is not so commonly described for tufas, although they also can be used as evidences of recent tectonic activity and if dated they can inform precisely of the timing of the neotectonic events (Peña et al., 2000; Pazzaglia et al., 2013).

The Quaternary Tortajada tufa studied in this paper (Fig.1A, B) is located in the eastern active margin of the Teruel semi-graben (Alonso-Zarza et al., 2012). Although the preserved deposit is relatively small, its longitudinal development perpendicular to main fault directions allows a complete characterization of the system. Through this study we pretend to: 1) show that the formation of these deposits occurred in well-constrained stages of evolution of the Teruel Graben, probably related to the initial stages of its opening; 2) discuss the role of the previous morphology of the basin in the distribution of sedimentary environment/facies and; 3) decipher the characteristics of the water and its probable sources. In sum to show that under suitable climatic conditions, tectonism may be a key control on the development of fluvial tufa, as it determines: the supply of water and solutes, and so location of the system; the morphology and situation of the different elements (cascades, ponds, etc...); and the vertical evolution of sedimentary sequences.

2. Geological setting

The Teruel Basin is a Neogene semi-graben situated within the Iberian Range (NE Spain). Its formation was linked to the Neogene-Quaternary Mediterranean rifting (Anadón et al., 1989; Ezquerro et al., 2014). This sedimentary basin with NNE-SSW direction is a half-graben whose active eastern margin is bounded by the Sierra de El Pobo mountain range, while the tilted western block (Sierra Palomera mountain range) (Fig.1A) forms its passive margin (Simón-Gómez 1983; Anadón and Moissenet 1996; Simón et al., 2012; Ezquerro et al., 2014). Basin margins are constituted by Triassic and Jurassic rocks, mostly carbonates and evaporites (Keuper facies). The Neogene basin is filled by 400-500 m of continental clastic, carbonate and evaporite deposits (Garcés et al., 1997; Alonso-Zarza and Calvo, 2000). During the Neogene and Quaternary the eastern margin of the basin was active, as shown by movement of the two main faults, Concud and Teruel. Both faults (mostly the Concud fault) were active with a continuous extensional movement during the Late Pliocene to Quaternary times, crosscutting previous Upper Miocene-Lower Pliocene deposits (Lafuente et al., 2011a, b) (Fig.1B).

From Lower-Middle Miocene to Middle Villafranchian (2 M.a), four erosion surfaces were recognized in the Iberian Range (Gracia-Prieto et al., 1988) shaping the Neogene relief. The last erosion surface, formed during the Middle Villafranchian, was slightly deformed due to extensional Quaternary movements (Peña et al., 1984; Gutiérrez and

Peña, 1990). The fluvial tufa system of Tortajada overlies this surface which formed prior to development of the Pleistocene terraces of the Alfambra and Guadalaviar Rivers (Gutiérrez and Peña, 1976; Peña et al., 1984). This surface postdates the last infill of the Neogene Teruel Basin (which behaved as a closed basin) and predate the entrenchment of the Alfambra River, and so, the opening of the basin. In the Alfambra River, three main fluvial terrace levels (disregarding the relatively recent terrace) were mostly developed on Miocene deposits. The age of lower and middle terraces are 15 ka and 169-90.5 ka respectively, whereas the age of the upper terrace is unknown (Gutiérrez and Peña, 1976; Peña et al., 1984; Lafuente et al., 2011b).

Some Pleistocene carbonate spring deposits occur in different positions all along the Alfambra River valley, following a mostly NNW-SSE direction. The northern-most is the Villalba Baja travertine which overlies Miocene deposits (Rodríguez-Berriguete et al., in press). Some others are located along the Concud fault overlying Pleistocene terraces (Lafuente et al., 2011b). These carbonates are dated between 116 ka and 169 ka. In addition, Lafuente et al. (2011b), also described a thin tufa deposit in Los Baños trench, in relation with a smaller fissure (see Fig.6 on Lafuente et al., 2011b).

3. Materials and methods

The extension of this fluvial tufa system, along with the considerable sedimentary, textural and spatial variability of these types of deposits, required large number of samples for a detailed study. Thus, 75 samples were collected in 3 periods of fieldwork, from November of 2011 to October of 2014.

During fieldwork, 5 sedimentary sections (Fig.6) were performed in some specific places. Collected samples were impregnated with epoxy resin due to their fragility. Petrological study was realized with thin sections in a conventional optical microscopy, using an Olympus BX51 petrological microscope.

Mineralogical semi-quantitative composition was determined by X-ray powder diffraction (XRD) using a Philips PW-1710 system operating at 40 KV and 30 mA, under monochromate CuKα radiation.

Microtextures and their smallest components were studied with gold-coated samples using FEI INSPECT (5350 NE Dawson Creek Drive, Hillsboro, Oregon 97124, USA) of the Museo Nacional de Ciencias Naturales (Madrid, Spain), operating with high vacuum mode (0.08 to 0.60 Torr) with conductive samples studied with both the large field detector (LFD) and backscatter detector (BSED-detector electron backscatter). SEM resolution at high vacuum was 3.0 nm at 30 kV (SE), 10 nm at 3 kV (SE), and 4.0 nm at 30 kV (BSE). Accelerating voltage was 20–30 kV, high vacuum 0.45 Torr, working distance of 10 mm.

For stable isotope analysis ($\delta^{13}C$ and $\delta^{18}O$), 28 samples were drilled for analysis at the Scientific and Technical Survey in Barcelona University (Spain). Samples were reacted with 100% phosphoric acid at 70°C for 3 min. CO_2 was extracted using a Thermo Finnigan Carbonate Kiel Device III isotopic analyzer with a Thermo Finnigan MAT-252 spectrometer, according to the McCrea (1950) method. $\delta^{13}C$ and $\delta^{18}O$ values, corrected using the NBS-19 standard and with an analytical precision of ±0.02‰ for $\delta^{13}C$ and ±0.04‰ for $\delta^{18}O$, are expressed in parts per thousand (‰) referring to VPDB standard.

4. Results

4.1. Description of Tortajada fluvial tufa. Morphology and location

The Tortajada fluvial tufa (TFT) occurs in a small area located in the eastern margin of the Teruel Basin (Fig.1A), about 3 km to E-NE from the closest point of the Concud fault. It is situated over mostly Triassic dolomitic limestones, marls and clays

(Muschelkalk and Keuper) in an area with important NE-SW normal faults (Fig.1B). The Triassic rocks are also cut by a network of secondary faults (NNW-SSE). The TFT probably developed after the formation of the last erosion surface. Its situation in relatively high areas suggests that they are the older fluvial Quaternary deposits found in the basin, probably Early Pleistocene in age. Initially it was connected to the Alfambra River, but both tectonic subsidence along the valley and fluvial incision has caused its final disconnection and dissection.

The Tortajada deposit was a fluvial tufa system which flowed downstream from E to W. The preserved deposit occurs in three different levels. From upstream to downstream are named as: Upper Terraces (formed by 3 terrace levels), middle Cascade-Ponds and Lower Terrace. This study is principally focused on the Upper Terraces and middle Cascade-Ponds.

At present, the Upper Terraces of the TFT are located approximately 1060 m to 1090 m a.s.l., situated about 150 m above the Alfambra River and composed of 3 terrace levels. The middle part consists of pond (approx. between 1050-1060 m a.s.l) and cascade deposits (approx. 1020-1050 m a.s.l.) distributed in two smaller waterfalls falling towards the west. The first waterfall is following the change in relief in relation with a NNE-SSW fault, while the second one is conditioned by a NNW-SSE fault. Finally, the Lower Terrace is poorly preserved (downstream towards the west, under the cascades) and overlies Miocene sediments.

4.2. Description and interpretation: facies, microfacies and microstructures

4.2.1. Framestone of stems (FST1 and FST2)

Description: This facies is formed mostly by curtains of calcified macrophyte and some bryophyte (mosses) hanging stems (FST1), growing downward. They occur in cascades and have the external morphology of speleothems. These curtains are about 1 m high and a few meters wide. Hanging stems are composed of: a) an internal part usually composed of macrophytes and some smaller bryophyte stems or fragments (Fig.2A), surrounded by crusts of small crystalline sparitic fans (<300 μm) with intercalations of thin micritic laminae (<40 μm) forming a laminated coating around stem moulds and, b) a thick external (approximately 0.4-1 cm) laminated cover (Fig.2A), formed by two microfacies. The first microfacies (2-4 mm thick) (not always present) grows perpendicularly to the calcified stems (described in the internal part) and includes reddish-translucent microlaminae (10-100 μm thick). It is formed by palisade calcite crystals (between 1-4 mm) (Fig.2B, D). The second outer microfabric (2-6 mm thick) consists of thin calcite bands (~150 μm thick) formed by calcite crystals with fan-like morphologies (~150 μm long), growing from thin micritic laminae (10-15 μm thick) (Fig.2B, C).

In some cases there are calcified stems of macrophytes growing upward (FST2). They occur in beds of 0.5 of 5 m width, up to 10 cm thick. Calcified stems can be longer than 2 cm long, with diameters of 2-3 mm. Under the microscope, macrophyte stems (moulds) are seen to be coated by laminated micrite/microsparite.

Interpretation: Framestones of stems grow downward (hanging stems) (FST1) forming the front of the barriers on vertical cascades. Small crystalline sparitic fans situated on the stems (either in internal or external parts) are interpreted as abiotic precipitation on the solid-water surface, during continuous water flow and rapid precipitation (Okumura et al., 2013b). Intercalated micritic laminae could be formed from decomposition of EPS which would induce precipitation of micritic crystals (Okumura et al., 2013a, b), by bacterial colonization on crystals when water flow is not too fast (Pedley, 1990; Janssen et al., 1999; Riding, 2008) or by degradation/micritization of previous larger calcite crystals, due to the input of under-saturated water (Martin-García et al., 2009).

The reddish-translucent microlaminae in the palisadic calcite suggest variations in water physicochemical or environmental conditions (Valero-Garcés et al., 2001) associated probably with seasonal changes (Jones and Renaut, 1994; Kano et al., 2003). Gradziński (2010) interpreted similar laminations as due to more rainy periods occurring during autumn. This would cause a decrease in SI_{calc} suggesting variations in growth rates during different precipitation episodes. In addition, Kano et al. (2004) suggested an increased in suspended clay concentration in response to various rainfall events which could generate reddish laminae. The presence of small amounts of organic matter (Freytet and Verrecchia, 1999) or iron oxides (Sanders et al., 2011) may also explain the origin of those reddish-translucent microlaminae, also indicating probable seasonal changes.

4.2.2. Phytoclastic rudstone (RP)

Description: Phytoclastic rudstone facies is composed of stem fragments of macrophytes (diameters from 1-2 mm to various centimeters) and bryophytes (diameter of <0.4 mm) (Fig.2E) embedded in micrite/microsparite matrix (Fig.2F). Phytoclastic rudstone facies is very porous, with intergranular (generally >1 cm pores) and intragranular porosity (generally <1 cm pores), the last one due to decomposition of stems (Fig.2E, F). Thickness of the poorly graded rudstone bodies range from decimeters to more than 1 meter.

Interpretation: Macrophyte and bryophyte fragment accumulation is the result of erosion of previous tufa deposits or vegetated areas by agitated waters with moderate to high water flow velocity (probably during flash-floods) (Pentecost, 2005; Arenas et al., 2010b; Gradziński et al., 2013), sometimes precipitating within conglomerate/sandstone fluvial deposits (see section 4.3 Sections and sequences). Even though rudstone of phytoclasts is a ubiquitous facies, it was generally deposited in calm water areas (e.g. dammed pools and palustrine areas), predominantly in local depressions within lobes, between bands of mosses (Gradziński et al., 2013), or in floodplains or barrage deposits (Vázquez-Urbez et al., 2012). Some of these quiet areas formed by obstacles or changes of relief that broke water flow, forming phytoclastic barrage rims and the core of barrages. Typically, the topmost part of phytoclastic barrage cores are covered by framestones of mosses or stromatolites (Arenas et al., 2010b).

4.2.3. Framestone of bryophytes (mosses) (FB)

Description: Framestones (phytoherms) of bryophytes commonly form thick wavy layers (1-6 cm), overlying other facies in small depressions (Gradziński et al., 2013). This facies is composed of thin stems of bryophytes (mosses) (usually >1 cm long, with diameter of approximately 0.3 mm) arranged parallel to each other (Fig.3A) and completely calcified by microsparite and coarse crystalline calcite (Fig.3B, C). These stems are arranged either perpendicularly or in parallel to the substrate. Pores left between individual bryophytes can reach up to 1 cm in diameter.

Large calcite crystals (>20 μm) containing small micritic bushes grow from thin secondary stems (<3 mm long with diameter <50 μm) (Fig.3C) developed from the central bryophyte stem (>1 cm long with diameter of approximately 0.3 mm) (Fig.3B) (similar to Fig.5E described by Gradziński et al., 2013). Brunched micritic bushes show the original structures of mosses (Fig.3C). Note also that the internal parallel structure of mosses is still preserved (Fig.3D).

Interpretation: Depending on water flow velocity, thin stalks of mosses can occur parallel or perpendicular to the surface and, therefore, to the paleo-flow, but in both cases precipitated in situ. Mosses have a wide range of tufa sub-environments in which they may appear, from calm palustrine zones to fast flowing stream areas (Pedley, 1990; Gradziński et al., 2013). Bryophytes usually appear in the uppermost part of cascades (associated barrages), in steps in low slope channels and sometimes also in pools and dammed areas, forming cushions (occasionally intercalated with phytoclasts) (Arenas et al., 2010b), in all cases, in illuminated areas of the tufa system.

4.2.4. Peloidal and filamentous stromatolites (S)

Description: This facies consist of stromatolitic bodies (from decimeters to 1.5 meters thick) with semi-planar morphology with slightly upward-convex tops (Fig.4A, B). Stromatolitic bodies are formed by layers (<5 cm thick) internally composed of thinner laminae (<1 cm thick). These laminae have internal peloidal layers (Fig.4C) (see 4.2.7 Granular and peloidal microfacies) intercalated with micritic masses. Besides, almost all stromatolitic laminations are linked to the presence of very small organic filaments (between 100-500 μm long and around 20 μm thick) (Fig.4D). These filaments, which are surrounded by microsparite, are either randomly distributed in a micritic matrix or growing from previous substrate to form stromatolitic laminations. In the last case, filaments are the support for the initial small-scale lamination (Fig.4D) before the formation of large-scale stromatolite bodies (Fig.4B). Stromatolitic facies occur on phytoclastic facies (described in 4.2.2 Phytoclastic rudstone) and under the central cascade bodies formed by hanging stems (described in 4.2.1 Framestone of stems FST1).

Interpretation: Stromatolites can form either in stagnant water or in fast flowing streams. Semi-planar stromatolitic bodies with internal peloidal laminae of the TFT represent a decrease in hydrodynamic energy (Casanova, 1994), with low-medium water flow velocity related with gently sloping zones. Organic filaments can provide a perfect biogenic site for calcite nucleation (Pentecost, 2005; Camuera et al., 2014), although these filaments are not always preserved (Guo and Riding, 1992). Their presence confirms the formation of this facies in waters with relatively low flow rates and weak agitation (Rainey and Jones, 2009).

4.2.5. Mudstone (M)

Description: Mudstone facies, composed mainly of micritic homogeneous matrix with less than 10% grains, occurs in beds with variable thicknesses, from a few centimeters to various decimetres. Mudstone are common in the eastern areas of the system (upstream). It contains charophytes, small plant moulds (mostly mosses) with diameters less than 0.5 mm, small bacterial filaments (<500 μm size), ostracods (<1.5 mm) some intraclasts, extraclasts and quartz grains (Fig.5A).

Interpretation: Mudstone with diverse biota can originate in dammed and low energy water areas protected from currents in floodplains, extensive shallow flats, or palustrine /shallow lacustrine micro-environments (Arenas et al., 2014b; Özkul et al., 2014). Homogeneous micrite precipitation is dominant in standing water between barrages (Arenas et al., 2010b) or in floodplains near the main watercourse (Vázquez-Urbez et al., 2012) and normally at the top of sequences (see 4.3 Sections and sequences). Coarse components were sourced either from recycling of previous tufa-like deposits (plant moulds and intraclasts) or from the surrounding reliefs.

4.2.6. Detrital deposits: Conglomerates (C) and Slope-breccias (SB)

Description: Two types of detrital deposits occur in the TFT. The first group is made up of cemented polymictic conglomerates (tufa and Mesozoic carbonate fragments and quartz) (from 2 mm to various centimeters size) and fine to coarse sands (0.1 mm to 2 mm size) with poor sorting. These conglomerates have rounded clasts with thin micritic oncoidal coatings and are cemented by fibrous phreatic calcite. They appear at the base of any sequence forming bodies of 1-1.5 m thickness and channel-like morphologies. The second group are slope-breccia deposits formed by angular clasts of Mesozoic carbonate, with sizes of up to 20 cm. Their sorting is poor, clast and/or matrix (micrite)-supported, structureless and lack grading. These breccias are intercalated mostly with phytoclastic rudstone tufa.

Interpretation: Conglomerate deposits come from the erosion of previous Mesozoic bedrock and nearby tufa deposits. These clasts were transported along fluvial systems during early stages of tufa formation, representing high discharge events (Vázquez-Urbez et al., 2012; Arenas et al., 2014b). Furthermore, the presence of gravels and sandstone related to stream channels suggest incision periods of the fluvial system (Vázquez-Urbez et al., 2012). Thus, they constitute the base of all the sedimentary sequences (channel, pond and cascade sequences) of the Tortajada fluvial tufa system (similar to described by Özkul et al., 2014). Breccias were formed by physical erosion of nearby Mesozoic carbonates, and some could reach the tufa system. Transport distance was very short, mostly by gravity transport and ephemeral flows (Alonso-Zarza et al., 1990) due to the high gradient slope of surrounding Mesozoic reliefs, representing slope or colluvial deposits that locally could reach the fluvial system.

4.2.7. Granular and peloidal microfacies (GPm)

Description: Granular and peloidal intraclastic microfacies are formed respectively by grains and peloids, coated by bladed and blocky microsparite/sparite cement (5-100 μm long) with thin micritic laminae (<20 μm thick). Granular microfacies are composed of carbonate grains (usually moss fragments) (between 0.5 mm and 1 cm size). Furthermore, peloids are micritic (between 0.1-0.5 mm size) (similar to Fig.6.8B from Viles and Pentecost, 2007), usually forming bands (<1 cm thick) intercalated with micritic masses (Fig.4C). Both granular microfacies and peloids appear within other facies, such as stromatolite facies (described in 4.2.4 Peloidal and filamentous stromatolites).

Interpretation: Granular microfacies probably formed by the mechanical fragmentation and transportation over short distances of framestone and micritic facies, although individualization of carbonate grains due to desiccation or biological bioturbation cannot be ruled out (Alonso-Zarza et al., 2012). In contrast, peloidal microfabric could be formed either by mechanical effects, bioturbation or remains of organisms (fecal pellets). Both types of components appear in calm and slow flowing water zones (dammed by barrages) (Arenas et al., 2014b) as also indicated by the micritic masses intercalated between peloidal bands. Coating of grains and peloids formed by sparitic/microsparitic laminae suggest that they were subject to phreatic processes.

4.2.8. Microbial microstructures (Mm)

Description: Well preserved microbial structures are randomly distributed on various facies, normally on the uppermost part of samples and normally associated with micritized masses (Fig.5B). These microbes are composed of thin filaments (<500 μm long and 5 μm thick) with circular connected spheres (diameters of 20 μm) (Fig.5C, D). Here we only refer to these special structures

Interpretation: In this study, the presence these of microbes always with micrite suggest the breakdown of previous calcite crystals by sparmicritization. This crystalline degradation indicates late diagenetic stages on the final morphology of microbially-involved facies (Kahle, 1977; Jones and Renaut, 2010). Other roles of microbes in carbonate precipitation have been discussed in stromatolitic facies (described in 4.2.4 Peloidal and filamentous stromatolites).

4.3. Sections and sequences

Logging of 5 detailed sections (Fig.6) along an eastern-western trend (downstream) revealed three main sedimentary sequences in the fluvial tufa system: channel sequence, pond sequence and cascade sequence (Fig.7).

From base to top, the terrace sequence is composed of fluvial conglomerates (C), phytoclastic rudstones (RP), stromatolitic facies (S) with granular/peloidal microfacies (GPm) and mudstones facies (M) (see Upper Terraces, S5 in Fig.6 and Fig.7).

Pond sequence has: fluvial conglomerates (C) at the base and mudstones (M) with phytoclastic sheets (RP) and bunches of stems growing upward (FST2) at the top. Sometimes gravels and breccias (SB) are also intercalated. In areas where low gradient slope steps/inter-barrages are formed, the sequence ends with stromatolites (S) and framestones of bryophytes (FB) (see Ponds/shallow lacustrine transitional system, S2 to S4 in Fig.6 and Fig.7).

The cascade sequence includes: fluvial conglomerates (C) at the base followed by phytoclastic rudstone (RP) with few intercalations of gravels and coarse sands (also some few clays). Stromatolite bodies (S) (with peloidal bands) occupy the middle part of the sequence. Hanging stems (FST1) and mudstones (M) with phytoclasts (RP) and framestone of bryophytes (FB) occur at the top (see Cascades, S1 in Fig.6 and Fig.7).

Interpretation:

All sequences have a base made up of conglomerates related to the initial fluvial incision, implying high energy and erosional episodes. As a rule the three sequences indicate a decrease in water energy.

Terrace sequence has phytoclastic deposits (over conglomeratic base), suggesting a reworking of previous macrophytes and bryophytes after fluvial incision. Stromatolitic sub-horizontal beds and granular/peloidal microfacies are indicative of shallow waters with low flow rates, associated with broad marginal zones in dammed terraces (Pedley et al., 1996) or forming the downstream and stepped side of barrages (Pedley, 1990). Finalizing with decreasing water-borne energy, upper mudstone facies represent stagnant inter-barrage areas protected from currents, where water was maybe deeper (Pedley, 1990; Arenas et al., 2010b).

The pond sequence deposited in relatively calm areas with low water flow velocity, allowed bunches of stems to grow up. Phytoclasts are ubiquitous facies which can be deposited during slow water flows or even due to a reworking of macrophytes during events with higher water velocity (Gradziński et al., 2013). Breccias appear randomly in some areas within mudstone facies suggesting erosional events of the nearby Mesozoic hillsides. As result, these slope-breccias are deposited into ponds or shallow lacustrine systems, mainly by gravitational processes (Alonso-Zarza et al., 1990). Stromatolites and framestones of bryophytes at the top of the sequence indicate the development of small steps in low gradient slope channels where thin water sheets flowed faster than during mudstone deposition.

The cascade sequence starts with phytoclasts and gravel/sand intercalations (overlying fluvial conglomerates) at the base. These initial deposits formed under moderate-high stream energy, although they can also present some fine-grained clastic deposits indicating calm periods. Sub-horizontal and undulated stromatolite bodies with internal peloidal bands indicate thin water sheets with low flow rate (Rainey and Jones, 2009). Nuclei of cascades are made up of thick bodies with hanging stems situated in jumps of the paleo-relief, which is formed as the result of active faulting (Lafuente et al., 2011a, b; Simón et al., 2012). Uppermost mudstone facies with phytoclasts and bryophytes were deposited in shallow and calm dammed areas with sporadically, some strong flood events. Thus, cascade sequence was conditioned by faulting activity (NNW-SSE secondary faults) which determined the presence of jumps in the river (Fig.7).

4.4. Mineralogy and geochemistry

Mineralogical analysis indicates between 92-100% of calcite in all samples. The remaining amount is quartz (<8%) and, in few samples, small amounts of gypsum and clays (<5%).

Isotopic values show slight variation in $\delta^{18}O$ (minimum of -8.58‰ VPDB and maximum of -6.70‰ VPDB), whereas $\delta^{13}C$ presents a wider range (minimum of -7.44‰ VPDB and maximum of -3.97‰ VPDB). Besides, the $\delta^{18}O$ covariance with $\delta^{13}C$ is low (Fig.8).

$\delta^{13}C$ values of cascade deposits (downstream zone) are slightly more positive than in the ponded area (upstream zone) (Fig.8B). Distance between these two areas is approximately 100 m. Within the same sub-environment the framestone of bryophyte facies show usually lower $\delta^{13}C$ values (Fig.8B). Hanging stems (described 4.2.1 Framestone of stems FST1) present also isotopic variations between the internal parts made up of macrophytes and bryophytes, and the external laminated covers which have heavier values in $\delta^{13}C$.

Interpretation

Common $\delta^{18}O$ and $\delta^{13}C$ for fluvial tufa carbonate deposits are between -5 and -8‰ PDB and -4 and -12‰ PDB, respectively (Andrews et al., 1997). Tortajada samples fall within these ranges, and are very similar to those of the Piedra and Mesa river tufas (Vázquez-Urbez, 2008; Arenas et al., 2010a) (Fig.8A). Negative isotope values are the result of meteoric water precipitated deposits, and also the input of dissolved ^{13}C-depleted CO_2 from the decay of organic matter in soil (Andrews et al., 1993). Low covariance in isotopic values is the result of a hydrologically open system with continuous water recharge and very short water residence in the system, leading to small fractionation of isotope (Andrews et al., 1997; Arenas et al., 2010b). Recharge of water was mostly surficial, but additional supplies from shallow-groundwater through the secondary faults (NNW-SSE) (Fig.7) are also considered.

$\delta^{18}O$ data indicate that the type of water involved in carbonate precipitation of the fluvial tufa (Janssen et al., 1999) was mainly inflowing meteoric water (Arenas et al., 2000; O'Brien et al., 2006) or that initial composition of waters throughout the system was poorly fractionated (mostly by abiogenic calcite precipitation). Low residence time in this open system reduced water evaporation (Andrews et al., 1997) and, therefore, prevented oxygen isotope fractionation, resulting in a poor covariance trend. Moreover, the scarce variation in $\delta^{18}O$ also suggests a fixed meteoric water composition (Talbot, 1990).

Carbon isotope data reflect the different processes occurring in fluvial tufa environments much more accurately. For example, $\delta^{13}C$ values are higher in cascade zones than in ponded areas due to preferential degassing of $^{12}CO_2$ downstream (Pentecost and Spiro, 1990; Andrews, 2006). Moreover, laminated external parts of hanging stems with heavier $\delta^{13}C$ suggest that these coatings precipitated from waters with longer residence times, favouring isotope fractionation, whereas internal parts of the hanging stems composed of macrophytes and bryophytes were probably calcified in a more open system, with higher water recharge and lower residence times. Thus the isotopic trend found in the hanging stems may reflect the initial stages of transition from cascade to pond formation, due to barrage growth.

Several studies have recorded an increase in the carbon isotopic signal linked to photosynthetic effects (Pentecost and Spiro, 1990; Lojen et al., 2004; García-del-Cura et al., 2014), but other studies have not observed this relation (Shiraishi et al., 2008). In this study, framestone of bryophyte (moss) facies present the lightest $\delta^{13}C$ values, which could be related to purely physicochemical precipitation. Bryophytes acted only as biogenic support for crystalline growth, so the biogenic signals of the samples involved has not been preserved. In contrast, heavy $\delta^{13}C$ values found in facies containing microbial features reflect the biogenic interaction of microbes with the crystals. The microbial organisms and other algae can remove isotopically light $^{12}CO_2$ during photosynthesis and respiration, enriching carbonate in ^{13}C (García-del-Cura et al., 2014).

5. Discussion

The Tortajada fluvial tufa developed in a very tectonically active area of the basin. Tectonic pulses have been controlling the sedimentation of the basin since the Miocene (Alonso-Zarza et al., 2012; Ezquerro et al., 2014). The system drained in E-W direction and it is at present disconnected of the present fluvial network due to differential tectonic movements that caused the incision of the Alfambra River. During Quaternary, the activity of different faults (Concud or Teruel) were the responsible of different intensity earthquakes (Lafuente et al., 2011a), and so the area has been seismically very active. Thus, E-W direction fault drove the incision of the system in Triassic rocks, while NNE-SSW and NNW-SSE faults were responsible of the different sub-environments within the system.

The location of three main areas of the system (Upper Terraces, middle Cascade-Ponds and Lower Terrace) responded to the morphology of the hinterland, which was also tectonically controlled. The Upper Terraces, formed during the initial incision of river entrenchment to form three levels, could have their origin in regional tectonic activity, including the movement of Concud and Teruel faults during Late Pliocene and early Quaternary (Lafuente et al., 2011a, b). These movements also created the scarp situated at present the east of the Tortajada lagoon, a favourable site for cascade formation whose aggradation could leave relatively flat/ponded areas behind. Downstream the cascades, the Lower Terraces formed on Miocene deposits. These irregularities in the longitudinal profile of fluvial tufa systems have been attributed to bedrock lithological characteristics (Meléndez et al., 1996; Sancho et al., 1997), in cases controlled by extensional tectonic activity as in the Mijares River (Spain) (Peña et al., 2000). Thus, the configuration of the overall TFT (Upper Terraces, Ponds and Cascades areas) responds to the location of the NNW-SSE secondary faults, which also acted as favourable conduits for water circulation. In short, tufas may behave similarly to travertines (Hancock et al., 1999) whose morphologies are controlled by both the local and the structural setting of the springs supplying the carbonate-rich waters.

Most of the sedimentary sequences of the Tortajada fluvial tufa have coarse detrital deposits at their bases, suggesting initial incision of the river. During the following stages (middle-top part of sequences), water-borne energy fell and carbonate sedimentation became widespread in ponded areas, allowing precipitation of mudstone facies and sub-horizontal stromatolites with peloids and organic filaments. Repetition of these sequences with time can be related to the varied entrenchment stages of the river, possibly due to small movements of faults and later stability phases allowing ponding. Similar interpretation has been done for the interbedding of external fluvial gravel and sand intervals with carbonate fluvial deposition in the Mijares River (Peña et al., 2000). Although similar trends could be also produced by channel migration, in this fluvial carbonate system the channels are relatively entrenched and the floodplain deposits are very scarce. This would make difficult the lateral migration of the channels.

The facies and the stable isotope results indicate that the TFT formed in a hydrologically open meteoric-water system. The system was fed by surface waters from high-mountain zones, and locally by shallow-groundwater upwelling across either bedding or fault plane discontinuities in the Mesozoic host-rock, as also described by Szulc et al., (2006) in the Triassic of Poland.

Similarly to other Pleistocene fluvial system in Spain (Pedley et al., 2003; Andrews, 2006; Arenas et al., 2014a, b), the TFT deposited under semi-arid climates, in which tufa deposition seems to be favored by warm conditions that characterize the odd-numbered isotopic stages (Pedley, 2009). The small size of the outcrop and the lack of precise chronological data make it difficult to assess the main development of this deposit to specific MIS periods. From our data it is not easy to infer how climatic variations could control the development of this system.

6. Conclusions

The deposition of the Pleistocene Tortajada fluvial tufa located in the marginal area of an active extensional basin, very probably was linked to the initial stages of opening of the Teruel Basin. The climatic conditions from semi-arid to sub-humid, together with the high amount of carbonates in the hinterland, favored carbonate sedimentation in the Pleistocene river, in spite of its situation in very proximal areas of the basin.

Different secondary faults outlined the paleomorphology of the river bed and so controlled the distribution of the different sedimentary environments and sequences. These faults created steps on which cascades developed, whereas behind them (upstream) pond and channel deposits were formed.

The varied sedimentary facies include framestones of stems, phytoclastic rudstone, framestone of bryophytes, peloidal and filamentous stromatolites, mudstone and detrital (conglomerates and slope-breccias) facies. All the carbonate facies are result of a complex interaction between biogenic and abiogenic processes, under different energy. In cases the biogenic components constitute the nucleation sites for late abiogenic precipitation (as in framestone of stems or in framestone of bryophytes), but in other cases microbes also alter the inorganic precipitates. The facies arrangement in all the environments indicates initial incision of fluvial network, subsequent development of ponded/shallow lacustrine areas, and formation of cascades on steps in the paleo-relief. These sequences are interpreted as the result of fault movements which cause an increase of the river gradient energy.

The Tortajada deposit, composed almost entirely of calcite, shows a low range of negative $\delta^{18}O$ values which indicate continuous meteoric water input and short residence time of water within a hydrologically open system. Upwelling of shallow-groundwater through faults is also considered, and could also determine the location of the overall system. Variations in $\delta^{13}C$ values (always negative) are higher than those of $\delta^{18}O$ and reflect the varied mechanisms of calcite precipitation.

Our study indicates that in some geological situations, such as basin margins of extensional basins, tufa deposits developed under a strong tectonic control. Tectonism does not only control, as in travertines, the water supply through faults, but also the paleomorphology and distribution of the sedimentary environments and the development of the different sedimentary sequences. In addition to tectonism, the formation of these fluvial carbonate in the margin of extensional basins also requires suitable climates and carbonate-dominated hinterlands.

7. Acknowledgements

We acknowledge the technical staff of the Museo Nacional de Ciencias Naturales from Madrid, with special thanks to Alberto Jorge García for helping us during the work on the Scanning Electron Microscope. Also to Carlos Liesa, Jose Luis Simón and Lope Ezquerro for their discussion during fieldwork. James Cerne for reviewing the English version of the manuscript and Antonio Grajera for the illustration. Finally, thanks to Mehmet Özkul and an anonymous reviewer for their corrections and suggestions. This work was funded by projects CGL2014-54818-P from the Spanish *Ministerio de Ciencia e Innovación* and UCM Research Group 910404.

8. References

Alonso-Zarza, A.M., Calvo, J.P., García-del-Cura, M.A., Hoyos, M., 1990. Los sistemas aluviales miocenos del borde NE de la cuenca de Madrid: sector Cifuentes-Las Inviernas (Guadalajara). Revista de la Sociedad Geológica de España 3, 213-229.

Alonso-Zarza, A.M., Calvo, J.P., 2000. Palustrine sedimentation in an episodically subsiding basin: the Miocene of the northern Teruel Graben (Spain). Palaeogeography, Palaeoclimatology, Palaeoecology 160, 1-21.

Alonso-Zarza, A.M., Meléndez, A., Martín-García, R., Herrero, M.J., Martín-Pérez, A., 2012. Discriminating between tectonic and climate signatures in palustrine deposits: Lessons from the Miocene of the Teruel Graben, NE Spain. Earth-Science Review 113, 141-160.

Anadón, P., Cabrera, L., Julia, R., Roca, E., Rosell, L., 1989. Lacustrine oil-shale basins in Tertiary grabens from NE Spain (Western European Rift System). Palaeogeography, Palaeoclimatology, Palaeoecology 70, 7-28.

Anadón, P., Moissenet, E., 1996. Neogene basins in the Eastern Iberian Range. In: Friend, P.F., Dabrio, C., (Eds.), Tertiary Basins of Spain. The Stratigraphic Record of Crustal Kinematics. World and Regional Geology Series 6, pp. 68-76.

Andrews, J.E., 2006. Palaeoclimatic records from stable isotopes in riverine tufas: synthesis and review. Earth-Science Reviews 75, 85-104.

Andrews, J.E., Riding, R., Dennis, P.F., 1993. Stable isotopic compositions of Recent freshwater cyanobacterial carbonates from the British Isles: local and regional environmental controls. Sedimentology 40, 303-314.

Andrews, J.E., Riding, R., Dennis, P.F., 1997. The stable isotope record of environmental and climatic signals in modern terrestrial microbial carbonates from Europe. Palaeogeography, Palaeoclimatology, Palaeoecology 129, 171-189.

Andrews, J.E., Pedley, M., Dennis, P.F., 2000. Palaeoenvironmental records in Holocene Spanish tufas: a stable isotope approach in search of reliable climatic archives. Sedimentology 47, 961-978.

Arenas, C., Gutiérrez, F., Osácar, C., Sancho, C., 2000. Sedimentology and geochemistry of fluvio-lacustrine tufa deposits controlled by evaporite solution subsidence in the central Ebro Depression, NE Spain. Sedimentology 47, 883-909.

Arenas, C., Cabrera, L., Ramos, E., 2007. Sedimentology of tufa facies and continental microbialites from the Palaeogene of Mallorca Island (Spain). Sedimentary Geology 197, 1-27.

Arenas, C., Osácar, C., Sancho, C., Vázquez-Urbez, M., Auqué, L., Pardo, G., 2010a. Seasonal record from recent fluvial tufa deposits (Monasterio de Piedra, NE Spain): sedimentological and stable isotope data. Geological Society, London, Special Publications 336, 119-142.

Arenas-Abad, C., Vázquez-Urbez, M., Pardo-Tirapu, G., Sancho-Marcén, C., 2010b. Chapter 3: Fluvial and Associated Carbonate Deposits. In: Alonso-Zarza, A.M., Tanner, L.H. (Eds.), Carbonates in continental settings: Facies, environments and processes. Developments in Sedimentology 61, pp. 133-175.

Arenas, C., Vázquez-Urbez, M., Auqué, L., Sancho, C., Osácar, C., Pardo, G., 2014a. Intrinsic and extrinsic control of spatial and temporal variations in modern fluvial tufa sedimentation: A thirteen-year record from a semi-arid environment. Sedimentology 61, 90-132.

Arenas, C., Vázquez-Urbez, M., Pardo, G., Sancho, C., 2014b. Sedimentology and depositional architecture of tufas deposited in stepped fluvial systems of changing slope: Lessons from the Quaternary Añamaza valley (Iberian Range, Spain). Sedimentology 61, 133-171.

Barnes, I., Irwin, W.P., White, D.E., 1978. Global distribution of carbon-dioxide discharges and major zones of seismicity. Geological Survey, Washington DC, United States.

Camuera, J., Alonso-Zarza, A.M., Rodríguez-Berriguete, A., Rodríguez-González, A., 2014. Origin and palaeo-environmental significance of the Berrazales carbonate spring deposit, North of Gran Canaria Island, Spain. Sedimentary Geology 308, 32-43.

Capezzuoli, E., Gandin, A., Sandrelli, F., 2010. Calcareous tufa as indicators of climatic variability: a case of study from southern Tuscany (Italy). Geological Society, London, Special Publications 336, 263-281.

Casanova, J., 1994. Stromatolites from the East African Rift: a synopsis. In: Bertrand-Sarfati, J., Monty, C. (Eds.), Springer Netherlands. Phanerozoic Stromatolites II, pp. 193-226.

Ezquerro, L., Luzón, A., Navarro, M., Liesa, C.L., Simón, J.L., 2014. Climatic vs. tectonic signals in a continental extensional basin (Teruel, NE Spain) from stable isotope ($\delta^{18}O$) and sequence stratigraphical evolution. Terra Nova 26, 337-346.

Ford, T.D., Pedley, H.M., 1996. A review of tufa and travertine deposits of the world. Earth-Science Reviews 41, 117-175.

Freytet, P., Verrecchia, E.P., 1999. Calcitic radial palisadic fabric in freshwater stromatolites: diagenetic and recrystallized feature or physicochemical sinter crust?. Sedimentary Geology 126, 97-102.

Gandin, A., Capezzuoli, E., 2008. Travertine versus calcareous tufa: distinctive petrologic features and stable isotopes signatures. Italian Journal of Quaternary Science 21, 125-136.

Garcés, M., Krijgsman, W., Van Dam, J., Calvo, J.P., Alcalá, L., Alonso-Zarza, A.M., 1997. Late Miocene alluvial sediments from the Teruel area: Magnetostratigraphy, magnetic susceptibility, and facies organization. Acta Geológica Hispánica 32, 171-184.

García-del-Cura, M.A., Sanz-Montero, M.E., De-los-Ríos, M.A., Ascaso, C., 2014. Microbial dolomite in fresh water carbonate deposits. Sedimentology 61, 41-55.

Gracia-Prieto, F.J., Gutiérrez-Elorza, M., Leránoz-Istúriz, B., 1988. Las superficies de erosión Neógenas en el sector central de la Cordillera Ibérica. Revista Sociedad Geológica de España 1, 135-142.

Gradziński, M., 2010. Factors controlling growth of modern tufa: results of a field experiment. Geological Society, London, Special Publications 336, 143-191.

Gradziński, M., Hercman, H., Jaskiewicz, M., Szczurek, S., 2013. Holocene tufa in the Slovak Karst: facies, sedimentary environments and depositional history. Geological Quarterly 57, 769-788.

Guo, L., Riding, R., 1992. Aragonite Laminae in Hot Water Travertine Crusts, Rapolano-Terme, Italy. Sedimentology 39, 1067-1079.

Gutiérrez, M., Peña, J.L., 1976. Glacis y terrazas en el curso medio del río Alfambra (provincia de Teruel). Boletín Geológico y Minero 87, 561-570.

Gutiérrez, M., Peña, J.L., 1990. Las formas del relieve de la Provincia de Teruel. Cartillas Turolenses 7, 64p.

Hancock, P.L., Chalmers, R.M.L., Altunel, E., Çakir, Z., 1999. Travitonics: using travertines in active fault studies. Journal of Structural Geology 21, 903-916.

Horvatinčić, N., Bronić, I.K., Obelić, B., 2003. Differences in the ^{14}C age, $\delta^{13}C$ and $\delta^{18}O$ of The Holocene tufa and speleothem in the Dinaric Karst. Palaeogeography, Palaeoclimatology, Palaeoecology 193, 139-157.

Janssen, A., Swennen, R., Podoor, N., Keppens, E., 1999. Biological and diagenetic influence in Recent and fossil tufa deposits from Belgium. Sedimentary Geology 126, 75-95.

Johnson, C.R., Ashley, G.M., De Wet, C.B., Dvoretsky, R., Park, L., Hover, V.C., Owen, R.B., McBrearty, S., 2009. Tufa as a record of perennial fresh water in a semi-arid rift basin, Kapthurin Formation, Kenya. Sedimentology 56, 1115-1137.

Jones, B., Renaut, R.W., 1994. Crystal fabrics and microbiota in large pisoliths from Laguna Pastos Grandes, Bolivia. Sedimentology 41, 1171-1202.

Jones, B., Renaut, R.W., 2010. Chapter 4: Calcareous Spring Deposits in Continental Settings. In: Alonso-Zarza, A.M., Tanner, L.H. (Eds.), Carbonates in continental settings: Facies environments and processes. Developments in Sedimentology 61, 177-224.

Kahle, C.F., 1977. Origin of subaerial Holocene calcareous crust: role of algae, fungi and sparmicritization. Sedimentology 24, 413-435.

Kano, A., Matsuoka, J., Kojo, T., Fujii, H., 2003. Origin of annual laminations in tufa deposits, southwest Japan. Palaeogeography, Palaeoclimatology, Palaeoecology 191, 243-262.

Kano, A., Kawai, T., Matsuoka, J., Ihara, T., 2004. High-resolution records of rainfall events from clay bands in tufa. Geology 32, 793-796.

Lafuente, P., Arlegui, L.E., Casado, I., Ezquerro, L., Liesa, C.L., Pueyo, O., Simón, J.L., 2011a. Geometría y cinemática de la zona de relevo entre las fallas neógeno-cuaternarias de Concud y Teruel (Cordillera Ibérica). Revista de la Sociedad Geológica de España 24, 1-2.

Lafuente, P., Arlegui, L.E., Liesa, C.L., Simón, J.L., 2011b. Paleoseismological analysis of an intraplate extensional structure: the Concud fault (Iberian Chain, eastern Spain). International Journal of Earth Sciences 100, 1713-1732.

Lojen, S., Dolenec, T., Vokal, B., Cukrov, N., Mihelcic, G., Papesch, W., 2004. C and O stable isotope variability in recent freshwater carbonates (River Krka, Croatia). Sedimentology 51, 361-375.

Luzón, M.A., Pérez, A., Borrego, A.G., Mayayo, M.J., Soria, A.R., 2011. Interrelated continental sedimentary environments in the central Iberian Range (Spain): Facies characterization and main palaeoenvironmental changes during the Holocene. Sedimentary Geology 239, 87-103.

Martín-García, R., Alonso-Zarza, A.M., Martín-Pérez, A., 2009. Loss of primary texture and geochemical signatures in speleothems due to diagenesis: Evidences from Castañar Cave, Spain. Sedimentary Geology 221, 141-149.

McCrea, J.M., 1950. On the isotopic chemistry of carbonates and paleotemperature scale. The Journal of Chemical Physics 18, 849-857.

Meléndez, A., Peña, J.L., Sancho, C., 1996. Factores fisicoquímicos que intervienen en el desarrollo de las barreras tobáceas bioconstruidas del río de la Fuente del Berro (Sierra del Albarracín, Teruel). Revista de la Sociedad Geológica de España 9, 125-134.

Muir-Wood, R., 1993. Neohydrotectonics. Zeitschrift Geomorphologie Supplementary 94, 275-284.

O'Brien, G.R., Kaufman, D.S., Sharp, W.D., Atudorei, V., Parnell, R.A., Crossey, L.J., 2006. Oxygen isotope composition of annually banded modern and mid-Holocene travertine and evidence of paleomonsoon floods, Grand Canyon, Arizona, USA. Quaternary Research 65, 366-379.

Okumura, T., Takashima, C., Kano, A., 2013a. Textures and processes of laminated travertines formed by unicellular cyanobacteria in Myoken hot spring, southwestern Japan. Island Arc 22, 410-426.

Okumura, T., Takashima, C., Shiraishi, F., Nishida, S., Kano, A., 2013b. Processes forming daily lamination in a microbe-rich travertine under low flow condition at the Nagano-yu hot spring, southwestern Japan. Geomicrobiology Journal 30, 910-927.

Ordóñez, S., García-del-Cura, M.A., 1983. Recent and Tertiary fluvial carbonates in Central Spain. Modern and ancient fluvial systems, 485-497.

Ortiz, J.E., Torres, T., Delgado, A., Reyes, E., Díaz-Bautista, A., 2009. A review of the Tagus river tufa deposits (central Spain): age and palaeoenvironmental record. Quaternary Science Reviews 28, 947-963.

Özkul, M., Kele, S., Gökgöz, A., Shen, C.C., Jones, B., Baykara, M.O., Fórizs, I., Németh, T., Chang, Y.W., Alçiçek, M.C., 2013. Comparison of the Quaternary travertine sites in the Denizli extensional basin based on their depositional and geochemical data. Sedimentary Geology 294, 179-204.

Özkul, M., Gökgöz, A., Kele, S., Baykara, M.O., Shen, C.C., Chang, Y.W., Kaya, A., Aratman, C., Akin, T., Örü, Z., 2014. Sedimentological and geochemical characteristics of a fluvial travertine: A case from the eastern Mediterranean region. Sedimentology 61, 291-318.

Pazzaglia, F., Barchi, M. R., Buratti, N., Cherin, M., Pandolfi, L., Ricci, M., 2013. Pleistocene calcareous tufa from the Ellera basin (Umbria, central Italy) as a key for an integrated paleoenvironmental and tectonic reconstruction. Quaternary International 292, 59-70.

Pedley, M., 1990. Classification and environmental models of cool freshwater tufas. Sedimentary Geology 68, 143-154.

Pedley, M., 2009. Tufas and travertines of the Mediterranean region: a testing ground for freshwater carbonate concepts and developments. Sedimentology 56, 221-246.

Pedley, M., Andrews, J., Ordóñez, S., García-del-Cura, M.A., Gonzáles-Martín, J.A., Taylor, M., 1996. Does climate control the morphological fabric of freshwater carbonates? A comparative study of Holocene barrage tufas from Spain and Britain. Palaeogeography, Palaeoclimatology, Palaeoecology 121, 239-257.

Pedley, M., González-Martín, J.A., Ordóñez-Delgado, S., García-del-Cura, M.A., 2003. Sedimentology of Quaternary perched springline and paludal tufas: criteria for recognition, with examples from Guadalajara Province, Spain. Sedimentology 50, 23-44.

Pentecost, A., 2005. Travertine. Springer, Berlin.

Pentecost, A., Spiro, B., 1990. Stable carbon and oxygen isotope composition of calcites associated with modern freshwater cyanobacteria and algae. Geomicrobiology Journal 8, 17-26.

Pentecost, A., Viles, H., 1994. A Review and Reassessment of Travertine Classification. Geographie Physique Et Quaternaire 48, 305-314.

Peña, J.L., Gutiérrez, M., Ibáñez, M.J., Lozano, M.V., Rodríguez, J., Sánchez, M., Simón, J.L., Soriano, A., Yetano, L.M., 1984. Geomorfología de la provincia de Teruel. Instituto de estudios Turolenses 149.

Peña, J.L., Sancho, C., Lozano, M.V., 2000. Climatic and tectonic significance of late Pleistocene and Holocene tufa deposits in the Mijares River canyon, eastern Iberian Range, northeast Spain. Earth Surface Processes and Landformns 25, 1403-1417.

Rainey, D.K., Jones, B., 2009. Abiotic versus biotic controls on the development of the Fairmont Hot Springs carbonate deposit, British Columbia, Canada. Sedimentology 56, 1832-1857.

Ricci, M., Bertini, A., Capezzuoli, E., Horvatinčić, N., Andrews, J.E., Fauquette, S., Fedi, M., 2014. Palynological investigation of a Late Quaternary calcareous tufa and travertine deposit: the case of study of Bagnoli in the Valdelsa Basin (Tuscany, central Italy). Review of Paleobotany and Palynology 218, 184-197.

Riding, R., 2008. Abiogenic, microbial and hybrid authigenic carbonate crusts: components of Precambrian stromatolites. Geologia croatica 61, 73-103.

Rodríguez-Berriguete, A., Meléndez, A., Alonso-Zarza, A.M., Martín-García, R., Martín-Pérez, A., (2015). El edificio Travertínico de Villaba Baja: un ejemplo de depósitos de surgencia en el Pleistoceno de la Fosa de Teruel (in press).

Rubio, J.C., Simón, J.L., 2007. Tectonic subsidence v. erosional lowering in a controversial intramontane depression: the Jiloca basin (Iberian Chain, Spain). Geological Magazine 144, 127-141.

Sancho, C., Peña, J.L., Meléndez, A., 1997. Control on the Holocene and present-day travertine formation in the Guadaliviar River (Iberian Chain, NE Spain). Zeitschrift fur Geomorphologie 41, 289-307.

Sanders, D., Wertl, W., Rott, E., 2011. Spring-associated limestones of the Eastern Alps: overview of facies, deposystems, minerals, and biota. Facies 57, 395-416.

Shiraishi, F., Zippel, B., Neu, T.R., Arp, G., 2008. In situ detection of bacteria in calcified biofilms using FISH and CARD–FISH. Journal of Microbiological Methods 75, 103-108.

Simón-Gómez, J.L., 1983. Tectónica y neotectónica del sistema de fosas de Teruel. Teruel: Revista del Instituto de Estudios Turolenses 69, 21-98.

Simón, J.L., Arlegui, L.E., Lafuente, P., Liesa, C.L., 2012. Active extensional faults in the central-eastern Iberian Chain, Spain. Journal of Iberian Geology 38, 127-144.

Szulc, J., Gradziński, M., Lewandowska, A., Heunisch, C., 2006. The Upper Triassic crenogenic limestones in Upper Silesia (south Poland) and their paleoenvironmental context. In: Alonso-Zarza, A.M., Tanner, L.H. (Eds.), Paleonvironmental Record and Applications of Calcretes and Palustrine Carbonates. Geological Society of America, Special Paper 416, 153-168.

Talbot, M.R., 1990. A review of the palaeohydrological interpretation of carbon and oxygen isotopic ratios in primary lacustrine carbonates. Chemical Geology: Isotope Geoscience section 80, 261-279.

Valero-Garcés, B., Arenas, C., Delgado-Huertas, A., 2001. Depositional environments of Quaternary lacustrine travertines and stromatolites from high-altitude Andean lakes, northwestern Argentina. Canadian Journal of Earth Sciences 38, 1263-1283.

Valero-Garcés, B.L., Moreno, A., Navas, A., Mata, P., Machín, J., Delgado-Huertas, A., González-Sampériz, P., Schwalb, A., Morellón, M., Hai Cheng, Edwards, R.L., 2008. The Taravilla lake and tufa deposits (Central Iberian Range, Spain) as palaeohydrological and palaeoclimatic indicators. Palaeogeography, Palaeoclimatology, Palaeoecology 259, 136-156.

Vázquez-Urbez, M., 2008. Caracterización y significado ambiental de depósitos tobáceos neógenos en la Cuenca del Ebro. Comparación con ambientes Cuaternarios. Ph.D. Thesis, Universidad de Zaragoza, Spain.

Vázquez-Urbez, M., Arenas, C., Pardo, G., 2012. A sedimentary facies model for stepped, fluvial tufa system in the Iberian Range (Spain): the Quaternary Piedra and Mesa valleys. Sedimentology 59, 502-526.

Viles, H.A., Pentecost, A., 2007. Chapter 6: Tufa and Travertine. In: Nash, D.J., McLaren, S.J. (Eds.), Geochemical Sediments and Landscapes. Blackwell Publishing, Oxford, pp. 173-199.

Figure captions

Fig.1: (A) Geographical map (upper left) showing the location of Teruel in the Iberian Peninsula and a schematic geological map (centre) of the Teruel semi-graben. Jiloca and Teruel basins are bounded by Mesozoic formations and determined by normal faults. The red square indicates the study area, detailed in Fig.1B. Modified from Rubio and Simón (2007) and Alonso-Zarza et al., (2012). (B) A detailed geological map of the red squared area of Fig.1A showing the location of the Tortajada fluvial-tufa system. Modified from IGME, 1981 (Magna 567, 27-22) and Lafuente et al., (2011a).

Fig.2: (A) Hand sample of hanging stems (1) coated by laminated calcite cover (2). (B) Microphotograph of the squared area of A, presenting two microfabrics which form the external laminated calcite cover. (C) Detail of B (squared C) showing the outer microfabric composed of bands with fan-like arrangement crystals. (D) Detail of B (squared D) showing the inner microfabric formed by palisade calcite crystals. (E) Hand sample of phytoclastic rudstone facies with high and irregular porosity distribution. (F)

Thin section of phytoclastic facies showing some bryophyte stems and micrite/microsparite matrix.

Fig.3: (A) Hand sample of framestone of bryophytes. (B) Detail and thin section of A (squared B) consisting of calcite crystals which grew on the bryophytes. Bryophytes are at the present decomposed. (C) Detail of B (squared C) showing the calcification of secondary bryophyte stems. Note that the original structure of the plant is still partially preserved (red arrows). (D) SEM image of the internal mould of bryophyte stem.

Fig.4: (A) Stromatolite facies presenting irregular convex-up morphologies. (B) Detail of A (squared B) showing stromatolite bodies composed of thin bands. (C) Peloidal layers presented in thin stromatolitic bands described in the previous photograph (Fig.4B). (D) Alternation of micrite/microsparite bands, growing from thin micrite filaments (red arrows).

Fig.5: (A) Thin section of mudstone facies showing small bryophyte moulds and an ostracod within a micritic matrix. (B) Thin section showing microbes in relation with micritized masses. (C) SEM image with microbes formed by connected circular spheres. (D) Detail of a SEM image which presents three circular spheres (microbial).

Fig.6: Sedimentary sections of the Tortajada fluvial tufa system. Sections from left (west and downstream) to right (east and upstream): Cascades (S1), Ponds/shallow lacustrine transitional system (S2, S3 and S4) and Upper Terraces (S5). See Fig.7 for its idealized situation.

Fig.7: Sketch showing paleogeographical reconstruction of the Tortajada fluvial tufa system and the location of the sedimentary sequences. S1 to S5 indicate the location of the sedimentary sections which are detailed in Fig.6.

Fig.8: Stable carbon and oxygen isotope composition of: (A) five different tufa deposits from the Iberian Peninsula (Arenas et al., 2007; Vázquez-Urbez, Thesis 2008 and

Arenas-Abad et al., 2010; Ortiz et al., 2009; Valero-Garcés et al., 2008; and present study) and four from other parts of the world (Andrews el a., 1993; Horvatinčić et al., 2003; Ricci et al., 2014; and Johnson et al., 2009). (B) Tortajada fluvial tufa samples separated by the Cascade sub-environment and Ponds/shallow lacustrine transitional sub-environment. Bryophyte samples are surrounded by a red circle.

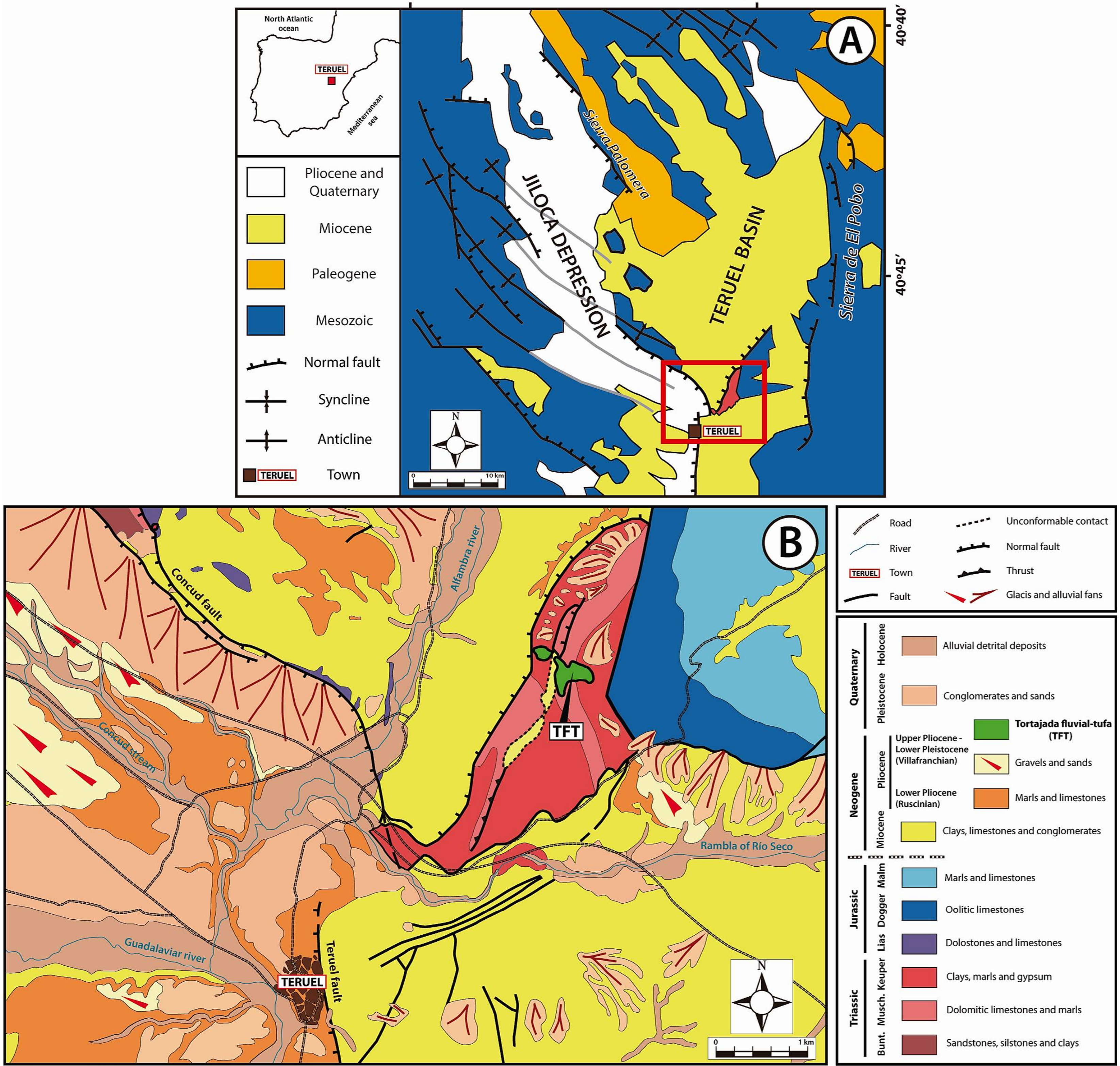
A
1°30′
1°00′
40°40′
40°45′
North Atlantic ocean
TERUEL
Mediterranean sea
Pliocene and Quaternary
Miocene
Paleogene
Mesozoic
Normal fault
Syncline
Anticline
TERUEL
Town
JILOCA DEPRESSION
Sierra Palomera
TERUEL BASIN
Sierra de El Pobo
N
0
10 km
B
Concud fault
Alfambra river
Concud stream
TFT
Rambla of Río Seco
Guadalaviar river
TERUEL
Teruel fault
N
0
1 km
Road
River
TERUEL
Town
Fault
Unconformable contact
Normal fault
Thrust
Glacis and alluvial fans
Quaternary
Holocene
Alluvial detrital deposits
Pleistocene
Conglomerates and sands
Neogene
Pliocene
Upper Pliocene - Lower Pleistocene (Villafranchian)
Tortajada fluvial-tufa (TFT)
Gravels and sands
Lower Pliocene (Ruscinian)
Marls and limestones
Miocene
Clays, limestones and conglomerates
Jurassic
Malm
Marls and limestones
Dogger
Oolitic limestones
Lias
Dolostones and limestones
Triassic
Keuper
Clays, marls and gypsum
Musch.
Dolomitic limestones and marls
Bunt.
Sandstones, silstones and clays

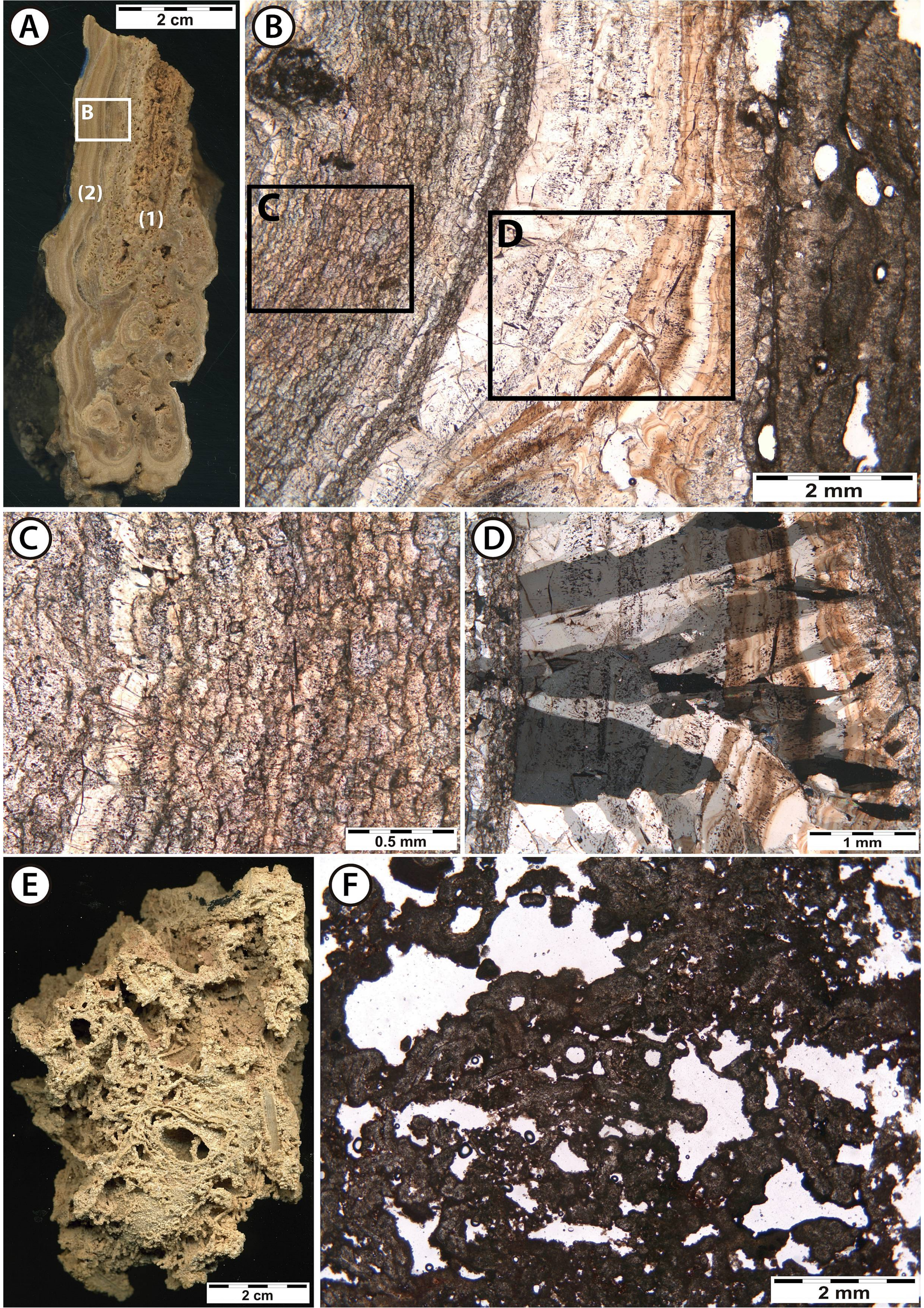
A
2 cm
B
(2)
(1)
B
C
D
2 mm
C
0.5 mm
D
1 mm
E
2 cm
F
2 mm

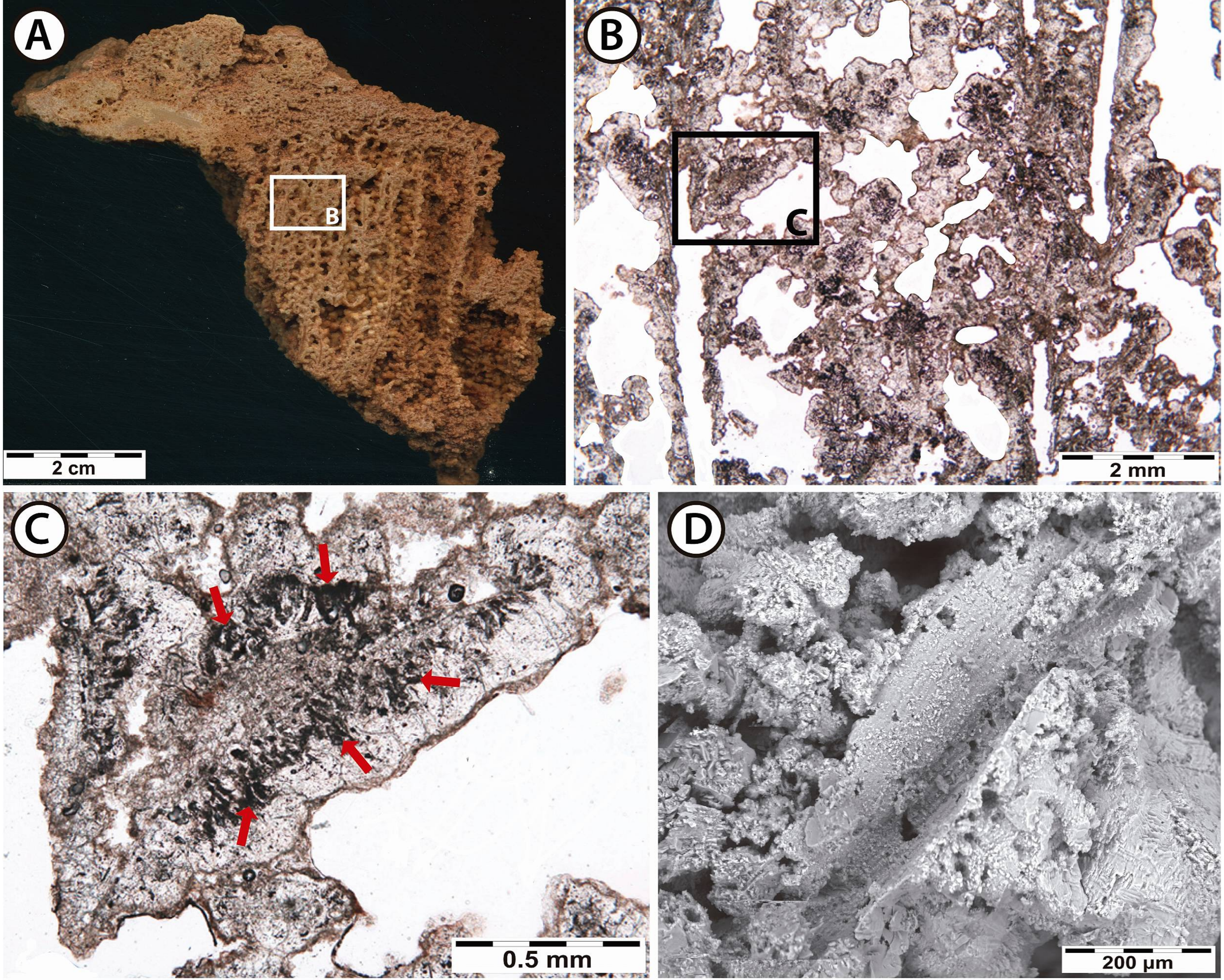
A
B
2 cm
B
C
2 mm
C
0.5 mm
D
200 µm

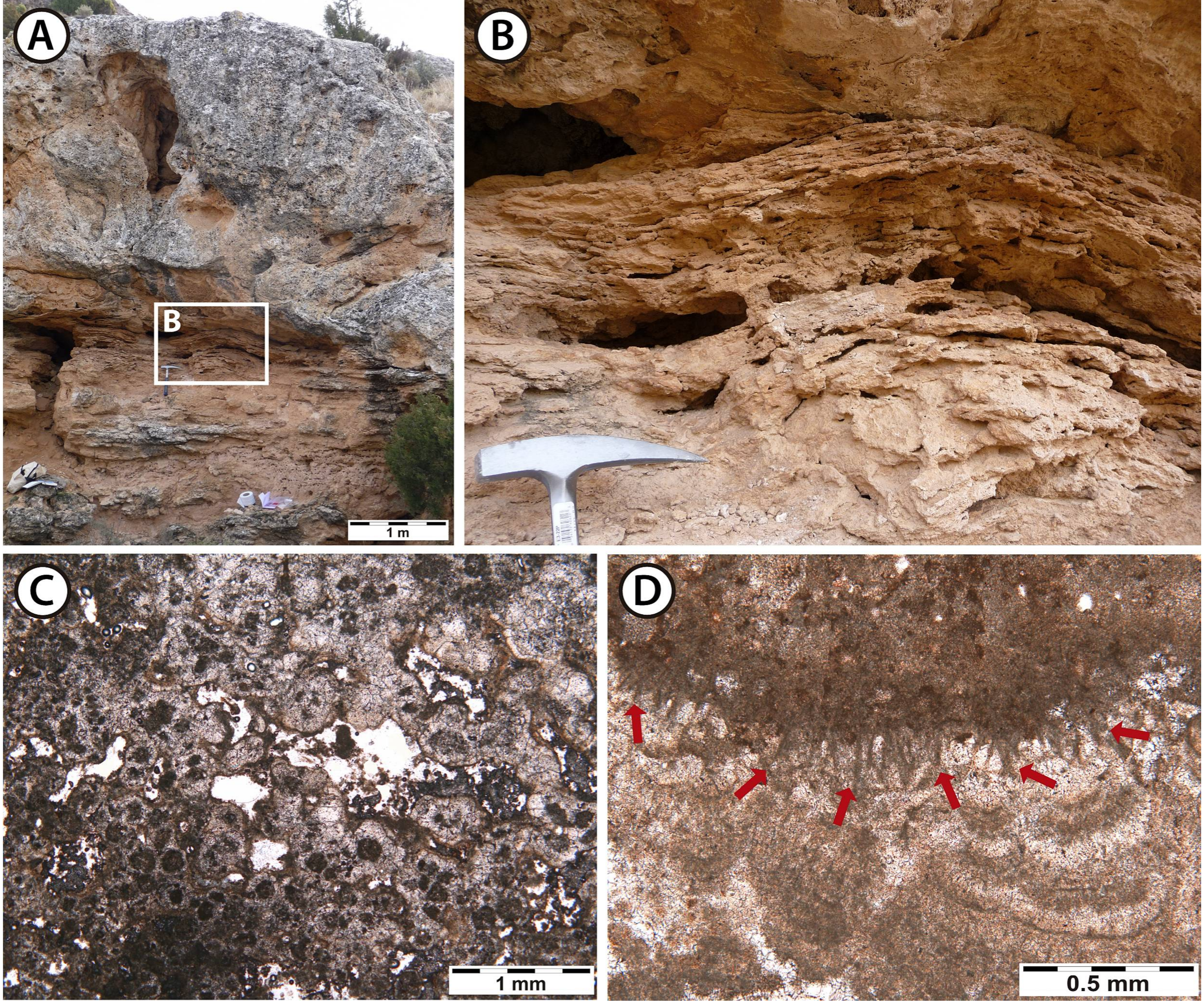
A
B
1 m
B
C
1 mm
D
0.5 mm

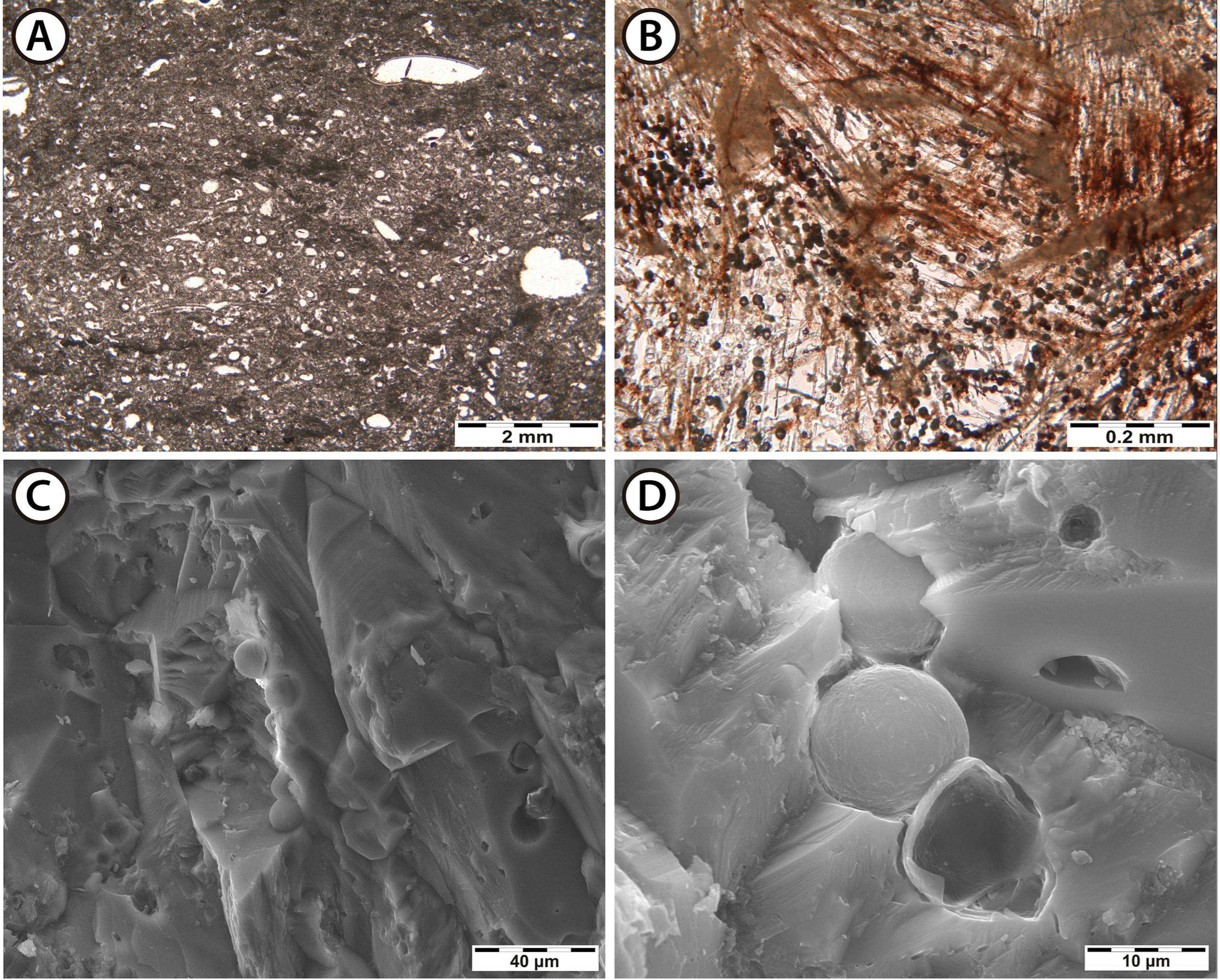
A
2 mm
B
0.2 mm
C
40 µm
D
10 µm

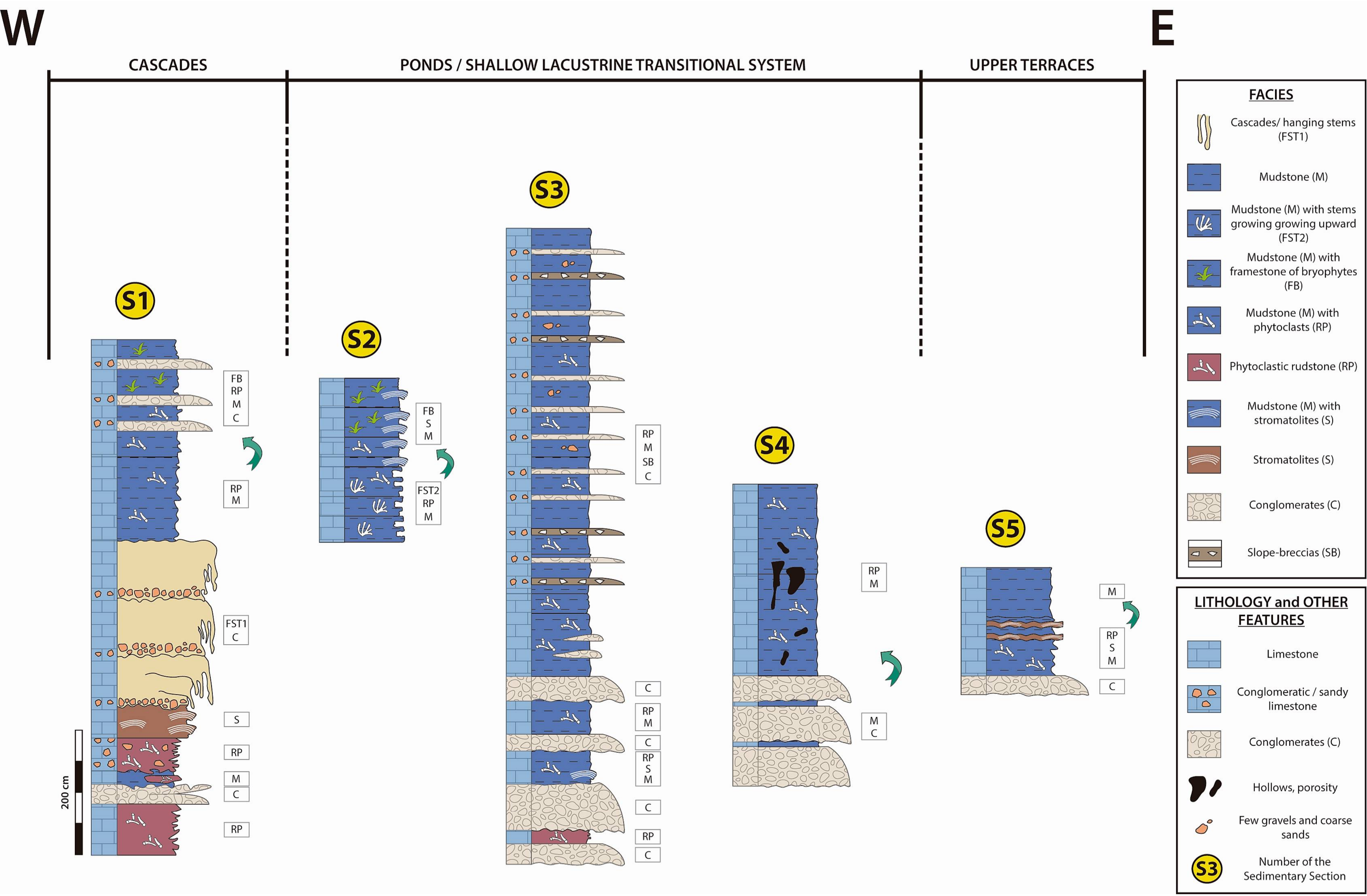
W
E
CASCADES
PONDS / SHALLOW LACUSTRINE TRANSITIONAL SYSTEM
UPPER TERRACES
S1
S2
S3
S4
S5
FB
RP
M
C
RP
M
FST1
C
S
RP
M
C
RP
200 cm
FB
S
M
FST2
RP
M
RP
M
SB
C
C
RP
M
C
RP
S
M
C
RP
C
RP
M
M
C
M
RP
S
M
C
FACIES
Cascades/ hanging stems (FST1)
Mudstone (M)
Mudstone (M) with stems growing growing upward (FST2)
Mudstone (M) with framestone of bryophytes (FB)
Mudstone (M) with phytoclasts (RP)
Phytoclastic rudstone (RP)
Mudstone (M) with stromatolites (S)
Stromatolites (S)
Conglomerates (C)
Slope-breccias (SB)
LITHOLOGY and OTHER FEATURES
Limestone
Conglomeratic / sandy limestone
Conglomerates (C)
Hollows, porosity
Few gravels and coarse sands
S3
Number of the Sedimentary Section

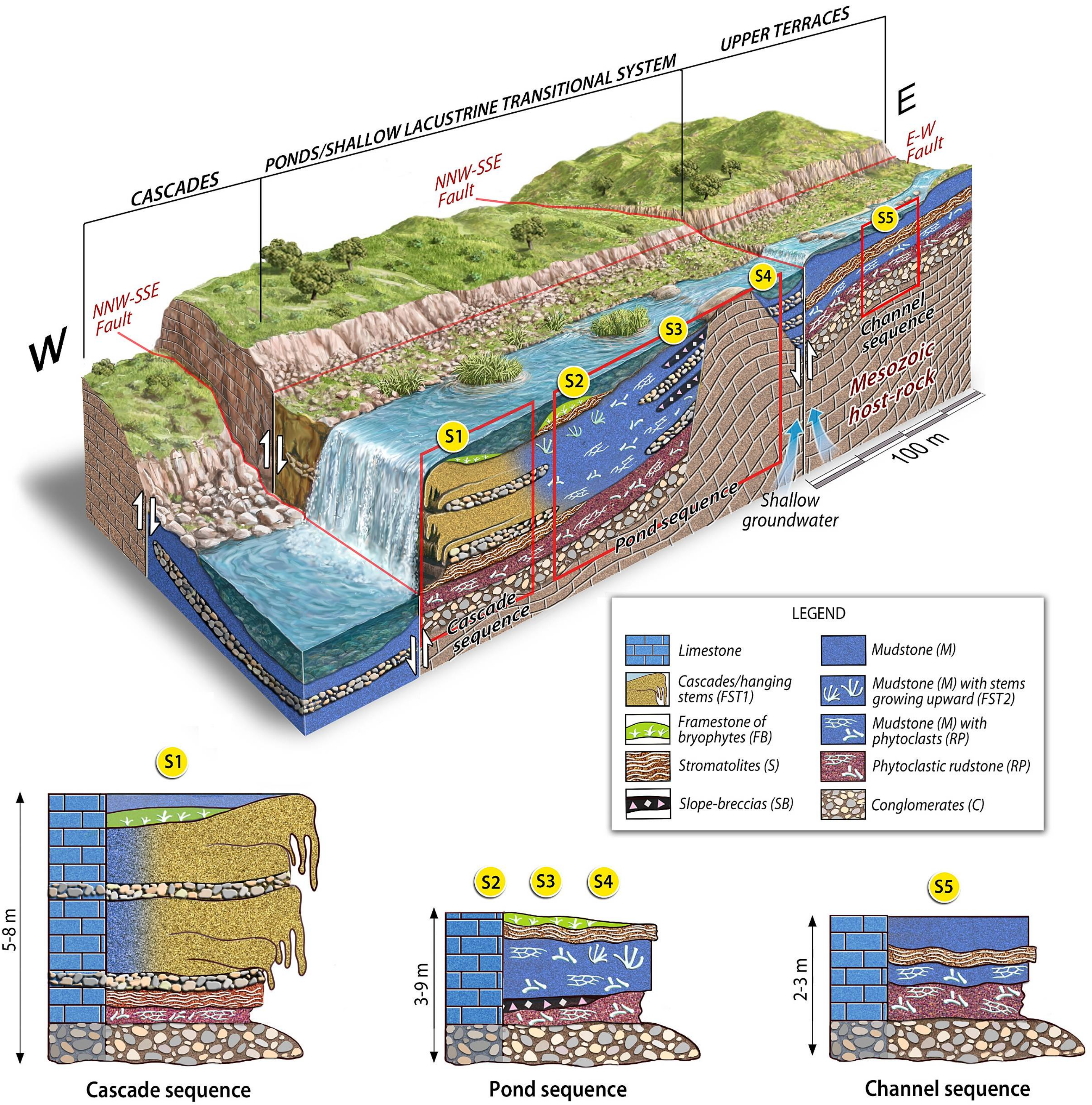
CASCADES
PONDS/SHALLOW LACUSTRINE TRANSITIONAL SYSTEM
UPPER TERRACES
W
E
NNW-SSE Fault
NNW-SSE Fault
E-W Fault
S1
S2
S3
S4
S5
Cascade sequence
Pond sequence
Channel sequence
Mesozoic host-rock
Shallow groundwater
100 m
LEGEND
Limestone
Cascades/hanging stems (FST1)
Framestone of bryophytes (FB)
Stromatolites (S)
Slope-breccias (SB)
Mudstone (M)
Mudstone (M) with stems growing upward (FST2)
Mudstone (M) with phytoclasts (RP)
Phytoclastic rudstone (RP)
Conglomerates (C)
S1
5-8 m
Cascade sequence
S2
S3
S4
3-9 m
Pond sequence
S5
2-3 m
Channel sequence

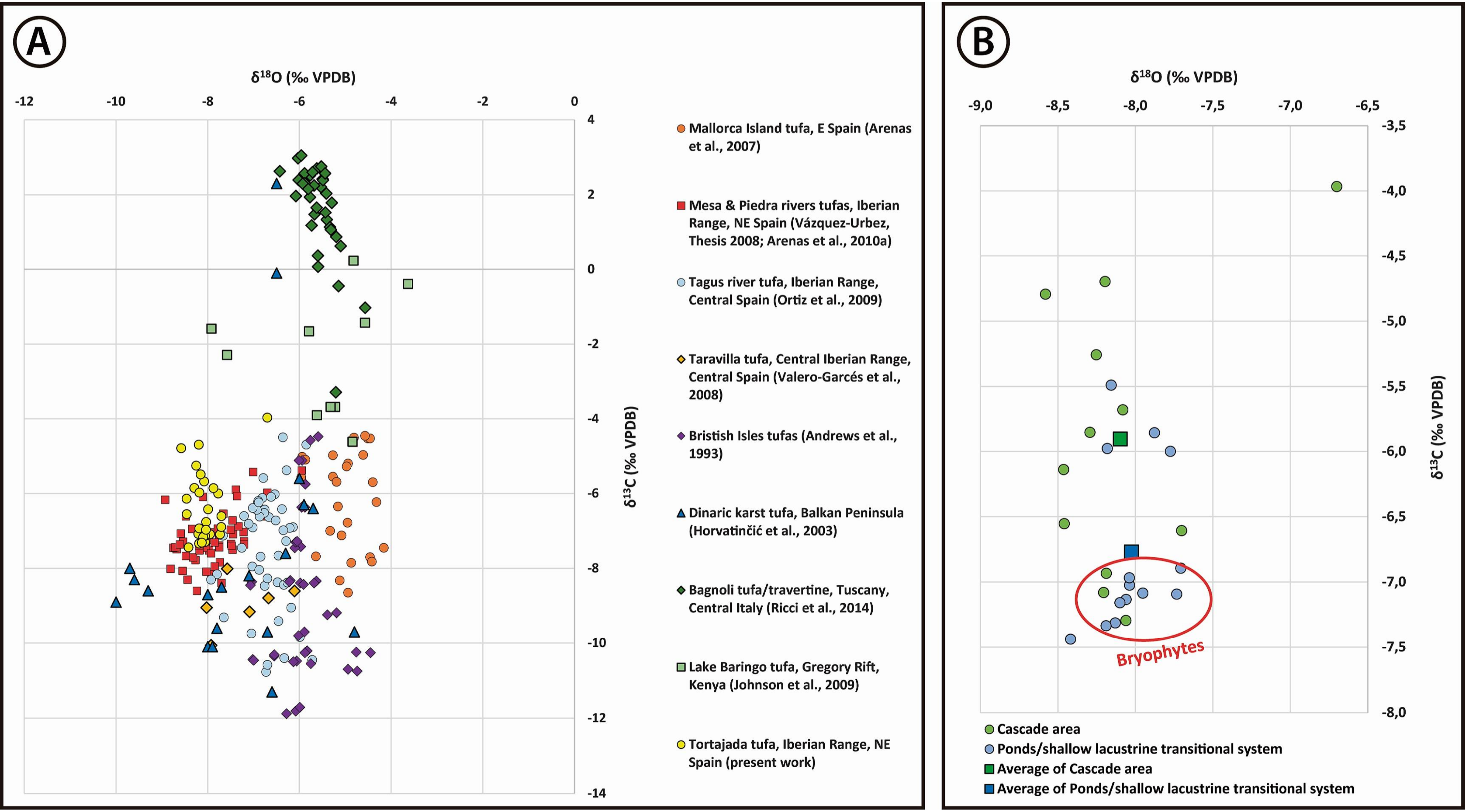
A
δ18O (‰ VPDB)
-12
-10
-8
-6
-4
-2
0
4
2
0
-2
-4
-6
-8
-10
-12
-14
δ13C (‰ VPDB)
Mallorca Island tufa, E Spain (Arenas et al., 2007)
Mesa & Piedra rivers tufas, Iberian Range, NE Spain (Vázquez-Urbez, Thesis 2008; Arenas et al., 2010a)
Tagus river tufa, Iberian Range, Central Spain (Ortiz et al., 2009)
Taravilla tufa, Central Iberian Range, Central Spain (Valero-Garcés et al., 2008)
Bristish Isles tufas (Andrews et al., 1993)
Dinaric karst tufa, Balkan Peninsula (Horvatinčić et al., 2003)
Bagnoli tufa/travertine, Tuscany, Central Italy (Ricci et al., 2014)
Lake Baringo tufa, Gregory Rift, Kenya (Johnson et al., 2009)
Tortajada tufa, Iberian Range, NE Spain (present work)
B
δ18O (‰ VPDB)
-9,0
-8,5
-8,0
-7,5
-7,0
-6,5
-3,5
-4,0
-4,5
-5,0
-5,5
-6,0
-6,5
-7,0
-7,5
-8,0
δ13C (‰ VPDB)
Bryophytes
Cascade area
Ponds/shallow lacustrine transitional system
Average of Cascade area
Average of Ponds/shallow lacustrine transitional system